Central European Journal of Energetic Materials, **2013**, *10*(3), 393-407
ISSN 1733-7178

Preparation and Characterization of Ultrafine RDX

Arti PANT*, Amiya Kumar NANDI,
Shireeshkumar Pralhad NEWALE, Vandana Prakash GAJBHIYE,
Hima PRASANTH and Raj Kishore PANDEY

Chemical Engineering & Pilot Plant Division, High Energy Materials Research Laboratory,
Sutarwadi, Pune-411021, Maharashtra, India
**Email: pant.arti@hemrl.drdo.in*

Abstract: This paper describes the synthesis of ultrafine Hexogen (UF-RDX) of size <5μm by drowning-out crystallization. RDX was precipitated from acetone or dimethylformamide (DMF) solution by reducing the solvent power using either a miscible, non-aqueous antisolvent, n-hexane, or an aqueous antisolvent, water containing polyethylene glycol (PEG). Process parameters such as solvent/antisolvent ratio, agitation, ultrasonication *etc*. were studied. UF-RDX was characterized for Brunauer-Emmett-Teller (BET) surface area, X-ray diffraction (XRD), Scanning Electron Microscope (SEM), Fourier Transform Infrared Spectroscopy (FT-IR), Differential Scanning Calorimetry (DSC) and sensitivity tests. In the case of the non-aqueous antisolvent, the precipitated RDX crystals were rod shaped of diameter <1 μm. For the aqueous antisolvent, oval shaped crystals (<5 μm) were precipitated. UF-RDX was found to be more sensitive to impact and less friction sensitive compared to production grade RDX (60-80 μm).

Keywords: ultrafine RDX, drowning-out crystallization, BET surface area, SEM, mechanical and electrostatic spark sensitivity

Introduction

Research Department Explosive (RDX) (chemical name cyclotrimethylene-trinitramine or 1,3,5-trinitro-1,3,5-triazacyclohexane; because of its cyclic structure and cyclonic nature, it is also known as 'cyclonite' in the USA. The Germans call it 'Hexogen' whilst the Italians call it 'T_4') is one of the widely

used military explosives. Fine particles (<30 μm) of RDX find applications in rocket and gun propellants, plastic bond explosive (PBX) formulations, low vulnerability ammunition [1], and in warhead fillings [1-8]. Accordingly, there has been a great deal of interest in the size reduction of production grade RDX (PG-RDX; 60-80 μm).

Different techniques have been attempted by various authors to realize fine explosive powders. These techniques include mechanical grinding [9-15], precipitation using suitable antisolvents [9-10, 16-18], spray drying [7, 19-22], supercritical fluid recrystallization [23-28], sol-gel [29] and reverse micelle [30]. In the milling technique, the particles are subjected to mechanical stress and this is therefore quite hazardous, which restricts the process to wet milling. Precipitation of RDX from acetone solution using water as the antisolvent gives fine particles (10-20 μm) [17, 18]. The Gas Antisolvent Process (GAS) and the Rapid Expansion of Supercritical Solution (RESS) process, using supercritical carbon dioxide, precipitate RDX in ultrafine (<5 μm) and submicrometer (<0.5 μm) particulate form respectively. However, the above processes have several disadvantages, such as high pressure (>70 bar) operation, difficulties in particle collection and downstream processing of the supercritical fluid. The sol-gel technique (precipitation of RDX in a silica matrix) incorporates silica impurity in the product and the process has limitations for scale up. A similar sol-gel concept was applied by Song *et al*. [31] who reported a method to realize nano RDX by dissolving amorphous iron oxide from a RDX/Fe_2O_3 aerogel using dilute hydrochloric acid. A direct method for the preparation of ultrafine RDX (5-10 μm) by changing the process conditions of hexamine nitration was also reported [32]. Chen *et al*. [33] reported a spray evaporation method which gave nanometer RDX (40-60 nm). Zhang *et al*. [34] reported the preparation of nano RDX by dispersing acetone solutions of RDX into stirred water. Dabin *et al*. [30] also reported preparation of nano-RDX (70-100 nm) by solvent substitution in reverse micelles. However, the authors did not mention the isolation methodology of the nano-RDX.

The present paper describes a low temperature (<5 °C) drowning-out crystallization method to realize UF-RDX (<5μm). Both non-aqueous and aqueous drowning-out crystallizations were attempted. RDX was precipitated from acetone or DMF solution by reducing the solvent power by the addition of miscible antisolvents such as n-hexane, cyclohexane, ethanol and water (containing 0.3% PEG). Process parameters such as solvent to antisolvent ratio, agitation, application of ultrasound *etc*. were studied. The precipitated product was characterized by BET surface area, FTIR, XRD, DSC, SEM, and sensitivity tests (friction, impact and electrostatic spark discharge).

Materials and Methods

Materials

PG-RDX, manufactured in Ordnance Factory, Bhandara, India, was used as the starting material. Acetone, N,N-dimethylformamide (DMF), n-hexane, cyclohexane, ethanol and PEG-200 (polyethylene glycol) were of synthesis grade from Merck (India) Ltd. Distilled water was used for all experiments.

Method

The drowning-out crystallization (precipitation) was carried out in a beaker (HDPE) or round bottomed flask at 1 g (RDX) per batch. The typical experimental method is described here: a measured quantity of antisolvent (n-hexane or water containing 0.3% PEG or cyclohexane or ethanol) was placed in a HDPE beaker (5 L) or round bottomed flask surrounded by ice-water in an ultrasonic bath (cap. 20 L). A mechanical stirrer (SS, impeller blade) was fitted into the beaker or round bottomed flask for agitation. RDX solution (1 g dissolved in 25 mL acetone or 10 mL DMF) was added to the antisolvent at a given rate from a graduated addition flask (similar to a separating funnel). The addition was carried out at low temperature (<5 °C) with application of mechanical stirring and ultrasonication. The agitation was continued for a given period after completion of the addition. The resultant slurry was filtered (Whatman filter paper No. 46), dried in the oven (50 °C) and then further characterized.

Characterization

Infrared spectra of the samples were recorded on a Thermonicolet FTIR spectrometer (Model Nicolet 5700, USA) using a KBr matrix. The BET surface areas of the powders were measured by nitrogen adsorption using a Gemini VII 2390t surface area analyzer (Micromeritics, USA).

The particle size was determined using a Malvern particle size analyzer (Mastersizer 2000, Malvern Instruments Ltd, UK). A small quantity of the RDX powder sample was dispersed in demineralized water (500 mL) with 2-3 drops of surfactant. The dispersed RDX was circulated in the measuring cell unit using the instrument's internal pumping system. The sample was dispersed using the instrument's internal stirring system (rpm ~2050) and with the help of an ultrasonic probe (USP). The sample was added in portions until the laser obscuration level was in the desired range (11-20%) as specified by the instrument manufacturer.

An environmental SEM (Model FEI Quanta 200 and 200 3D, Eindhoven, The Netherlands) was used for particle imaging. The RDX powder was mounted

on double sided adhesive conducting silver tape pasted on Al stub.

Differential Scanning Calorimetry (DSC) was carried out using a Perkin Elmer DSC instrument (DSC-7). Approximately 1-3 mg sample in a crimped aluminium pan was heated from 50 °C to 300 °C under a nitrogen atmosphere at 10 °C/min.

The powder X-ray diffraction (XRD) of the RDX samples was carried out using an X-ray difractometer (Bruker D8 advance) with a Cu Kα source for an angle range 2θ = 20-50° at a scan rate of 2 °/min.

Friction sensitivity was determined using a Julius Peter apparatus and impact sensitivity by the fall hammer method (Bruceton staircase method. Height of 50% (H_{50}) explosion was determined with 2 kg drop weight).

An in-house designed electrostatic spark discharge apparatus [35] was used to determine the spark sensitivity of fine RDX powder. The stored energy ($E= ½ CV^2$; *C* is the capacitance in Farad, *E* the energy in Joules, and *V* is the charging voltage in volts) is discharged to the sample through a spark gap. Ignition or deflagration behaviour of the sample was observed under a specific energy discharge. The energy discharged is gradually decreased either by changing the value of the capacitor or the voltage or by a combination of both as required until no ignition or deflagration occurs for the sample, in five consecutive experiments.

Results and Discussion

Supersaturation in a drowning-out crystallization system

Crystallization is a basic technique in process technology. It can be brought about either by cooling a saturated solution (cooling crystallization) or evaporation of a solvent component (evaporative crystallization) or reducing the solubility (solvent power) of a particular solvent-solute system by introducing an appropriate antisolvent (drowning-out or displacement crystallization). All of these techniques are widely used in industry to realize the product of a desired particle size [9, 10]. The particle size, distribution and shape of crystal can be controlled by recrystallization (cooling or evaporative crystallization, drowning-out crystallization). The degree of supersaturation is the key factor in the process [9, 36, 37].

Crystallization comprises of two important mechanisms *viz*. nucleation and crystal growth. Nucleation occurs when the solution equilibrium is disturbed under supersaturated conditions. Molecules or ions from the supersaturated solution attach themselves to the surface of the crystal nucleus and cause it to

grow. The introduction of an antisolvent into the system rapidly reduces the solubility of the solute and thus supersaturation develops in the system, which in turn induces nucleation with the formation of tiny crystals. These tiny crystals grow further and later precipitate. Rapid reduction in solubility creates a high nucleation rate. Hence, all of the tiny nuclei do not get an opportunity for further crystal growth and are precipitated as fine particles.

Precipitation of RDX from an acetone solution using water as an antisolvent is an industrially adopted method [17, 18] it gives particle size around 15 μm. It is difficult to reduce the particle size further by this method due to the inherent limitation of the process. Though water is quite capable of reducing the solvent power to a large extent, it's other properties such as polarity, dipole moment *etc*. do not arrest the crystal growth to the extent required to realize particle sizes of less than 10 μm. When PEG-200 (0.3%) was mixed with water and used as the antisolvent, it was found that the crystal growth rate was inhibited and generated UF-RDX.

Unlike water, n-hexane is a non-polar solvent in which RDX has a solubility almost equal to zero. It is also miscible with acetone. Hence, a very high supersaturation is created by the addition of an RDX solution (in acetone) to n-hexane. Low temperature operation reduces the rate of evaporation of the highly volatile solvent n-hexane. The low temperature also narrows down the metastable zone width (also known as the metastable limit) resulting in rapid nucleation which favours the formation of fine particles [36]. Hence, a detailed study (described in subsequent subsections) was carried out in order to understand the influence of various process conditions on the drowning-out crystallization.

Study of different solvent/antisolvent systems on particle size

RDX solutions were prepared in two different solvents *viz.* acetone and DMF. Drowning-out crystallization was attempted with 4 different antisolvents, *viz*., water (0.3% PEG solution), n-hexane, cyclohexane and ethanol. The particle size of the product was monitored by measurement of the BET surface area. The average particle size of the precipitated product was calculated from the BET surface area data (assuming that the particles are closed spheres with a smooth surface and of uniform size). The results are shown in Table 1. The BET surface area of the parent RDX was measured as 0.22 m^2/g and the corresponding average particle size was 15 μm. This particle size data, calculated from the BET surface area data, does not match with the actual particle size of PG-RDX (60-80 μm). This may be due to the non-spherical nature of the particles. However, BET surface area measurement was found to be effective in monitoring the particle size of the precipitated RDX.

Table 1. Precipitation of RDX from different antisolvent-solvent systems

Sample	Antisolvent-solvent system	Antisolvent /solvent ratio	Rate of solution addition [mL/h]	BET surface area (SA) [m^2/g]	Average particle size [μm] from SA data	Yield [%]
1.	Water (with 0.3% PEG)-acetone	125	50	1.16	2.8	68
2.	Water (with 0.3% PEG)-DMF	300	40	1.73	1.8	65
3.	Cyclohexane-acetone	34	50	1.46	2.5	81
4.	n-Hexane-acetone	34	50	1.7	1.9	77
5.	n-Hexane-DMF	40	40	0.51	6.4	86
6.	Ethanol-acetone	125	40	Precipitation did not occur		

Note: RDX conc. in acetone 40 g/L; DMF 100 g/L; temp. = ~5 °C; ultrasonication at 45 kHz; stirrer = 2000 rpm; Average particle size = 6000/(SA * d), SA = BET surface area in m^2/g and d = density of RDX (1.82 g/cc).

The water-acetone system with a volume ratio ~100 (sample 1) gave particle size ~2.8 μm. When the solvent was changed to DMF and the antisolvent/ solvent ratio increased to 300, the particle size was reduced further to 1.8 μm (sample 2).

Table 2. Results of precipitated RDX for various antisolvent-solvent ratios (BET surface area and average particle size)

Sample	Antisolvent/ solvent ratio	Rate of solution addition [mL/h]	Stirrer rpm	BET surface area [m^2/g]	Average particle size [μm] from BET data	Yield [%]
7.	5	25	1000	0.82	4.0	90
8.	10	17	1000	0.98	3.3	87
9.	20	25	1500	1.31	2.5	83
10.	30	25	1500	1.68	1.96	72
11.	100	50	2000	3.88	0.85	60

Note: solvent = acetone; antisolvent = n-hexane; RDX conc. in acetone 4 g/100 mL; Temp. = ~5 °C; ultrasonication at 45 kHz; Average particle size = 6000/(SA * d), SA =BET surface area in m^2/g and d = density of RDX (1.82 g/cc).

Three non-aqueous antisolvents, *viz*., n-hexane, cyclohexane and ethanol were tested. For the n-hexane-DMF system, with an antisolvent/solvent ratio ~40 (sample 5), the particle size was 6.4 μm. When the solvent was changed to acetone, the particle size was further reduced to ~1.9 μm (sample 4). n-Hexane was found to be a better antisolvent than cyclohexane (samples 4 and 3 respectively) in generating UF-RDX of lower particle size. Precipitation did

not occur with the ethanol-acetone system even at a high antisolvent/solvent ratio (~125). This may due to poor reduction in the solubility of RDX by the antisolvent ethanol. In fact, RDX is sparingly soluble in ethanol.

The effect of the n-hexane/acetone ratio on the product particle size is shown in Table 2. A higher antisolvent/solvent ratio gave finer particles. The highest BET surface area of the precipitated product was obtained with the antisolvent/solvent ratio of 100 (sample 11). The corresponding particle size was 0.85 μm.

FT-IR study

The FT-IR spectra of the precipitated RDX were found to match reported data [38]. The observed transmittance bands are: 1592 cm^{-1} ($\nu_s NO_2$); 1268 cm^{-1} ($\nu_s NO_2$ + νN-N); 1040 and 947 cm^{-1} (ring stretching); 783 cm^{-1} (δ and γ NO_2); 605 cm^{-1} (τ + γ NO_2) [24, 31]. There was no change or shift in the transmittance bands for UF-RDX samples when compared with those of the PG-RDX. This indicates that the chemical structure of RDX remains intact during precipitation and no impurity is incorporated in the UF-RDX.

Particle size analysis

The average particle size of the precipitated product was calculated from the BET surface area data (as described in Tables 1 & 2). However, a few samples were also analysed using a Malvern instrument. The particle size data are summarized in Table 3. The different types of average particle size and range are shown in the table. The average particle size for UF-RDX was much lower than that of PG-RDX. The lowest particle size (D[3,2] = 2.3 μm) was obtained for sample 11 (n-hexane-acetone system with ratio ~100). The typical particle size distribution curve for UF-RDX is compared with PG-RDX (Figure 1). UF-RDX shows a broad bimodal, size distribution compared to the narrow unimodal size distribution for PG-RDX.

Table 3. Average particle size data for RDX samples

Sample code	Average particle size, [μm]*			
	D [4,3]	D [3,2]	d [0.5]	Span
PG- RDX	62.5	44.8	58.2	1.3
UF-RDX (water/DMF at ratio 300, sample 2)	14.5	4.5	11.8	2.4
UF-RDX (n-hexane/acetone at ratio 20, sample 9)	12.8	4.1	10	2.6
UF-RDX (n-hexane/acetone at ratio 100, sample 11)	5.6	2.3	4.3	2.4

*D [4,3]: volume-weighted mean dia.; D [3,2]: surface-weighted mean dia.; d [0.5]: median dia.

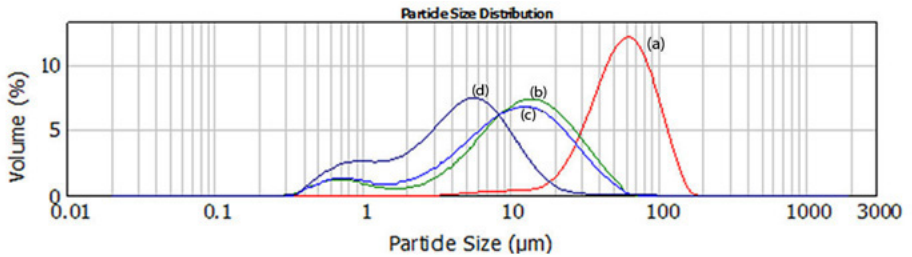

Figure 1. Particle size distribution curves for: (a) PG-RDX; (b) UF-RDX (water-DMF at ratio 300, sample 2); (c) UF-RDX (n-hexane-acetone at ratio 20, sample 9); (d) UF-RDX (n-hexane-acetone at ratio 100, sample 11).

Thermal study

The thermal study of the precipitated RDX was carried out using DSC. The DSC profile of UF-RDX samples was compared with that of PG-RDX (Figure 2). All of the DSC curves show a sharp endothermic peak at ~203 °C and a wide exothermic peak at ~239 °C. These correspond to the melting and decomposition of solid RDX respectively. These peaks match reported data [26, 39]. Frolov *et al.* [40] reported a decrease in melting temperature for nano RDX. However, we did not observe any change or shift in the DSC profile of UF-RDX when compared with that of PG-RDX.

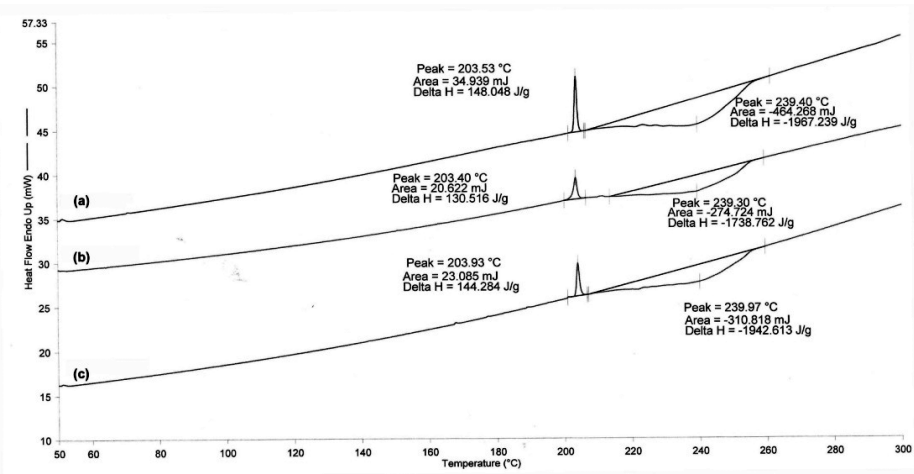

Figure 2. DSC profile of RDX samples: (a) PG-RDX ; (b) UF-RDX (n-hexane-acetone at ratio 100, sample 11); (c) UF-RDX (water-DMF at ratio 300, sample 2).

X-Ray Diffraction (XRD) study

XRD scans of RDX samples are shown in Figure 3. All peaks (2θ values) match those of standard RDX (PDF No. 00-005-0576). There is no change in the peak positions for UF-RDX samples compared to PG-RDX. This indicates the uniformity in crystallographic phase in all samples [41]. However, a change in peak intensities was observed when compared with PG-RDX. This may be due to different crystal habits and the finer particle size of UF-RDX [42].

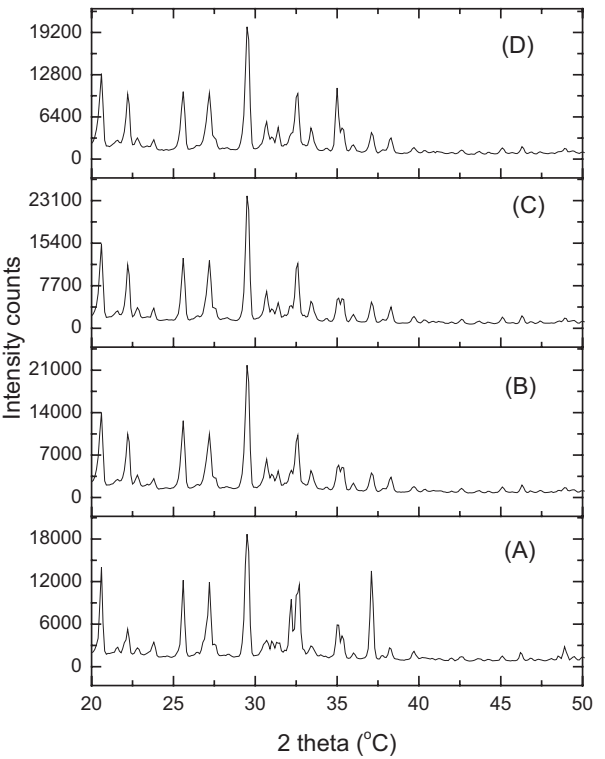

Figure 3. XRD profile for RDX samples: (a) PG-RDX ; (b) UF-RDX (water-DMF at ratio 300, sample 2); (c) UF-RDX (n-hexane-acetone at ratio 20, sample 9); (d) UF-RDX (n-hexane-acetone at ratio 100, sample 11).

SEM study

The SEM photograph of a PG-RDX sample showed irregular shaped crystals with rough surfaces (60-80 μm, Figure 4a). The UF-RDX particles showed different morphologies depending upon the antisolvent/solvent system used. UF-RDX particles obtained from the n-hexane-acetone system (sample 9) were

of irregular shape, *viz.,* rods, cylinders (with some branches and curves), ovals (Figure 4b). However, at a higher antisolvent/solvent ratio (100), the UF-RDX (sample 11) had a rod-shaped crystal morphology (Figure 4c; diameter <1 μm and length <20 μm). Lee *et al.* [16] reported the formation of rod-like micrometer RDX particles (diameter ~2-5 μm and length 15-20 μm) using the same antisolvent-solvent system. However, we observed a rod diameter in the submicrometer range. This may be due to the high antisolvent/solvent ratio with effective macromixing (mechanical agitation) and micromixing (ultrasonication). However, when the solvent/antisolvent system was changed to DMF-water, the precipitated RDX (sample 2) particles (<5 μm) were found to be oval shape (Figure 4d).

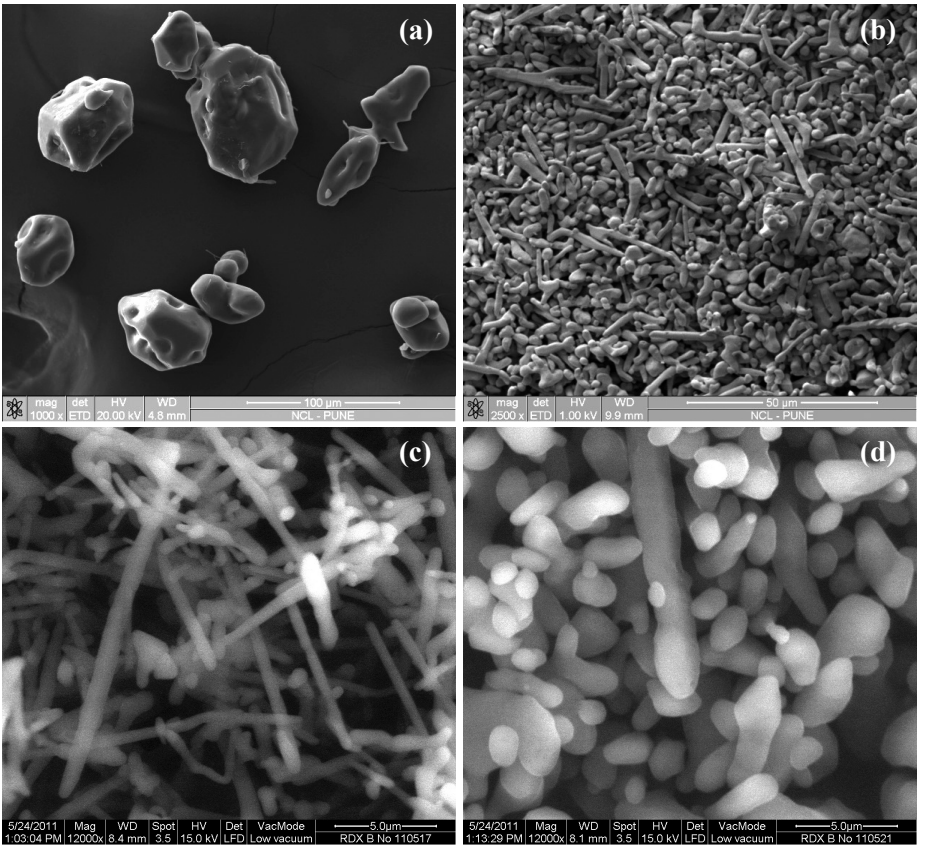

Figure 4. SEM images of RDX samples: (a) PG-RDX; (b) UF-RDX (n-hexane:acetone at ratio 20, sample 9); (c) UF-RDX (n-hexane:acetone at ratio 100, sample 11); (d) UF-RDX (water-DMF at ratio 300, sample 2).

Sensitivity tests

Friction and impact sensitivity data of the RDX samples are given in Table 4. It is observed that the UF-RDX is more impact sensitive (7.4 J) than PG-RDX (8.6 J). However, the friction sensitivity has been improved in precipitated RDX. Zeman *et al*. [43] have reported a semi-logarithmic relationship between friction and impact sensitivity of different fractions of HMX. According to them, decreasing the particle size resulted in a decrease in the friction sensitivity and an increase in the impact sensitivity. A similar trend is also observed here. The friction force during shearing is proportional to the contact area of the explosive particles [44]. The rod shape particles give a lower contact area for shearing which results in lower friction sensitivity. It was observed that the UF-RDX obtained from the DMF-water system is more insensitive to friction compared to that from the acetone-n-hexane system. This may be due to the round shaped morphology of the crystals [45, 46]. However, a more detailed study is essential in order to give a valid explanation of the above experimental observations.

Table 4. Impact and friction sensitivity data for RDX samples

No.	Sample	Impact sensitivity for 50% explosion [J]	Insensitivity to friction [N]	Temp. [°C]	RH [%]
1	PG- RDX	8.6	235.3	26	55
2	UF-RDX (water/DMF at ratio 300, sample 2)	7.4	353	26	55
3	UF-RDX (n-hexane/acetone at ratio 20, sample 9)	7.4	353	32	20
4	UF-RDX (n-hexane/acetone at ratio 100, sample 11)	7.4	294.2	26	55

Spark or ESD sensitivity data are summarised in Table 5. UF-RDX was found to be less sensitive to spark when compared to PG-RDX. Generally fine particles of any explosive become more sensitive to spark when compared with coarse one [47-48]. However, the reverse was observed in this case. This may be due to the different morphology of UF-RDX (rod-shaped).

Table 5. Spark/ESD sensitivity for RDX samples

Sample	C [μF]	V [kV]	E [mJ]	Temp. [°C]	RH [%]	Remarks
PG- RDX	0.01	8.6	370	32.5	40	not ignited
UF-RDX (water/DMF at ratio 300, sample 2)	0.01	8.6	370	32.5	35	not ignited
UF-RDX (n-hexane/acetone at ratio 20, sample 9)	0.01	9.0	405	30.5	48	not ignited
UF-RDX (n-hexane/acetone at ratio 100, sample 11)	0.01	10.0	500	32.5	40	not ignited

C: Capacitance; V: Voltage; E: Energy at spark gap where no ignitions were observed for five consecutive experiments.

Conclusions

The non-aqueous and aqueous drowning-out crystallization method was developed to synthesize UF-RDX. Non-aqueous precipitation (at a very high antisolvent/solvent ratio ~100) gives rod-shaped crystals with a rod diameter in the submicrometer range (<1 μm). Oval shaped (<5 μm) crystals are precipitated with the aqueous antisolvent. Though the drowing-out crystallization methodology did not lead to precipitation of nano-RDX, the precipitated products were ultrafine in nature, and may be useful for application as an energetic ingredient in propellant formulations. The sensitivity studies indicated that the precipitated material was more sensitive to impact and less sensitive to friction.

Acknowledgements

The Project team acknowledges the guidance and encouragement given by Shri B. Bhattacharya, Outstanding Scientist and Director, HEMRL, to carry out this research work. The Project team also acknowledges the support rendered by various divisions of HEMRL, such as CAID (SEM), EMR (FTIR and DSC), INST (ESD), Pyro (Friction and Impact sensitivity). Support extended to us by National Chemical Laboratory (NCL), Pune, for SEM analysis is also acknowledged.

References

[1] Pillai A.G.S., Sanghavi R.R., Dayanandan C.R., Joshi M.M., Velapure S.P., Singh A., Studies on RDX Particle Size in LOVA Gun Propellant Formulations, *Propellants Explos. Pyrotech.*, **2001**, *26*, 226-228.

[2] Muller D., Helfrich M., *Stabilized Explosives and Its Production Process*, US 5026443, June **1991**.

[3] Siviour C.R., Gifford M.J., Walley S.M., Proud W.G., Field J.F., Particle Size Effects on the Mechanical Properties of a Polymer Bonded Explosive, *J. Mater. Sci.*, **2004**, *39*, 1255-1258.

[4] Pivkina A., Ulyanova P., Frolov Y., Zavyalov S., Schoonman J., Nanomaterial for Heterogeneous Combustion, *Propellants Explos. Pyrotech.*, **2004**, *29*, 39-48.

[5] Manning T.G., Strauss B., *Reduction of Energetic Filler Sensitivity in Propellants through Coating*, US 6524706 B1, February **2003**.

[6] Luman J.R., Wehrman B., Kuo K.K., Yetter R.A., Masoud N.M., Manning T.G., Harris L.E., Bruck H.A., Development and Characterization of High Performance Solid Propellants Containing Nano-sized Energetic Ingredients, *Proc. Comb. Inst.,* **2007**, *31*, 2089-2096.

[7] Qiu H., Stepanov V., Stasio A.R.Di., Chou T., Lee W.Y., RDX Based Nanocomposite Microparticles for Significantly Reduced Shock Sensitivity, *J. Hazard. Mater.*, **2011**, *185*, 489-493.

[8] Brown L.G., *High Energy Gun Propellant*, US 6241833 B1, June **2001.**

[9] Teipel U., *Energetic Materials: Particle Processing and Characterization*, Wiley-VCH, Verlag GmbH, Weinheim, Germany, **2000**.

[10] Teipel U., Production of Particles of Explosives, *Propellants Explos. Pyrotech*., **1999**, *24*, 134-139.

[11] Narani M.S., Tavangar S., Motamedalshariaty S.H., Fathollahi M., Ghaeni H., Seyednaseredini S.M., Hoseini S.G., Production of Nano-RDX by Wet Batch Ball Milling, *Proceedings of the 2007 International Autumn Seminar on Propellants, Explosives and Pyrotechnics*, Xi'an, Shaanxi, China, **2007**, p. 18-19.

[12] Estabrook L.C., Somoza C., *Wet Grinding of Crystalline Energetic Materials*, US 5197677, March **1993**.

[13] Patel R., Cook P., Crane C., Redner P., Kapoor D., Grau H., Gandzelko A., *Production and Coating of Nano RDX Using Wet Milling*, NDIA IM/EM 10/15/07.

[14] Redner P., Kapoor D., Patel M., Chung M., Martin D., *Production and Characterization of Nano RDX*, U.S. Army, RDECOM-ARDEC Picatinny, NJ, **2006**.

[15] Teipel U., Mikonsaari I., Size Reduction of Particulate Energetic Materials, *Propellants Explos. Pyrotech.,* **2002**, *27*, 168-174.

[16] Lee K-Yin., Laintz K.E., *RDX Explosion and Method*, US 2009/0107593 A1, **2009**.

[17] Saha K.K., Wani P.M., Ramprasad S.V., Size Reduction of RDX Particles to Low Micron Range in Constant Flow Stirred Tank Reactor (C.F.S.T.R), *Colloquium on*

Chemical Engineering and Process Development, HEMRL, Pune, India, **1994**, 248.

[18] Wani P.M., Saha K.K., Ramprasad S.V., Size Reduction of RDX Particles to Low Micron Range by Eduction, *Colloquium on Chemical Engineering and Process Development*, HEMRL, Pune, India, **1994**, 263.

[19] Radacsi N., Stankiewicz A.I., Creyghton Y.L.M., van der Heijden A.E.D.M., ter Horst J.H., Electrospray Crystallization for High Quality Submicron Crystals, *Chem. Eng. Technol.,* **2011**, *34*, 624-630.

[20] Mercado L., Torres P.M., Gomez L.M., Mina N., Hernández S.P., Lareau R., Chamberlain R.T., Castro-Rosario M.E., Synthesis and Characterization of High Energy Nanoparticles, *J. Phys. Chem. B.*, **2004**, *108*, 12314-12317.

[21] Spitzer D., Baras C., Schafer M.R., Ciszek F., Siegert B., Continuous Crystallization of Submicrometer Energetic Compounds, *Propellants Explos. Pyrotech*., **2011**, *36*, 65-74.

[22] Kim J-Woo., Shin M-Soo., Kim J-Kyeong, Kim H-Soo., Koo K-Kahb., Evaporation Crystallization of RDX by Ultrasonic Spray, *Ind. Eng. Chem. Res*., **2011**, *50*, 12186-12193.

[23] Gallagher P.M., Coffey M.P., Krukonis V.J., Klasuits N., Gas Anti-solvent Recyrstallization: New Process to Recrystallize Compounds Insoluble in Supercritical Fluid, *ACS Symp. Ser*., **1989**, *406*, 334-354.

[24] Teipel U., Kröber H., Krause H.H., Formation of Energetic Materials Using Supercritical Fluids, *Propellants Explos. Pyrotech*., **2001**, *26*, 168-173.

[25] Stepanov V., Krasnoperov L.N., Elkina I.B., Zhang X., Production of Nanocrystalline RDX by Rapid Expansion of Supercritical Solutions, *Propellants Explos. Pyrotech*., **2005**, *30*, 178-183.

[26] Lee B.-M., Jeong J.-S., Lee Y.-H., Lee B.-C., Kim H.-S., Kim H., Lee Y.-W., Supercritical Antisolvent Micronization of Cyclotrimethylenetrinitramine: Influence of the Organic Solvent, *Ind. Eng. Chem. Res*., **2009**, *48*, 11162-11167.

[27] Pourmortazavi S.M., Hajimirsadeghi S.S., Application of Supercritical Carbon Dioxide in Energetic Material Processes: A Review, *Ind. Eng. Chem. Res.,* **2005**, *44*, 6523-6533.

[28] Essel J.T., Cortopassi A.C., Kuo K.K., Leh C.G., Adair J.H., Formation and Characterization of Nano Sized RDX Particles Produced Using the RESS-AS Process, *Propellants Explos. Pyrotech*., **2012**, *37*, 699-706.

[29] Tillotson T.M., Hrubesh L.W., Simpson R.L., Lee R.S., Swansiger R.W., Simpson, L.R. Sol-Gel Processing of Energetic Materials, *J. Non-Cryst. Solids*, **1998***, 225*, 358-363.

[30] Dabin L., Dong X., Baochang Z., Jinhua P., Yaolin G., Qinwen F., Preparation of Nanometer RDX In-situ by Solvent Substitution Effect in Reverse Micelles, *26th International Pyrotechnics Seminar,* Nanjing, PR China, **1999**, 1-4 Oct, p. 269.

[31] Song X.-L., Li F.-S., Zhang J.-L., Wang Y., An C.-W., Guo X.-D., Preparation, Mechanical Sensitivity and Thermal Decomposition Characteristics of RDX Nanoparticles, *Chinese J. Explos. Propellants*, **2008***, 31,* 1-4.

[32] Rui J.H., Feng S.S., Xu G.G.**,** A Direct Method of Preparing Ultra-Fine RDX

Crystals, *Journal of Beijing Institute of Technology*, **2001**, *21*,786-788.
[33] Chen H.H., Meng Q. G., Cao H., Pei Y. M., Zhu L.F., Lv C.X., Preparation and Impact Sensitivity of Nanometer Explosive Powder of RDX, *Explosion and Shock Waves*, **2004**, *24*, 382-384.
[34] Zhang Y.-X., Lü Ch.-X, Liu D.-B., Preparation of RDX Microcrystals with Nanometer Size by Recrystalization, *Chinese J. Explos. Propellants*, **2005**, *28,* 49-51.
[35] Talawar M.B., Agrawal A.P., Anniyappan M., Wani D.S., Bansode M.K., Gore G.M., Primary Explosives: Electrostatic Discharge Initiation, Additive Effect and Its Relation to Thermal and Explosive Characteristics, *J. Hazard. Mater.*, **2006**, *137*, 1074-1078.
[36] Myerson A.S. (Ed.), *Handbook of Industrial Crystallization*, Butterworth-Heinemann, Boston, **1993**, p. 18.
[37] Mullin, J.W., *Crystallization*, 4th ed. Rev., Butterworth-Heinemann, Oxford, UK, **2001**.
[38] da Costa Mattos E., Moreira E.D., Diniz, M.F., Dutra R.C.L., da Silva G., Iha K., Teipel U., Characterization of Polymer Coated RDX and HMX Particles, *Propellants Explos. Pyrotech*., **2008**, *33*, 44-50.
[39] Li F., Song X., Dependence of Particle Size and Size Distribution on Mechanical Sensitivity and Thermal Stability of Hexahydro-1,3,5-trinitro-1,3,5-triazine, *Def. Sci. J*., **2009**, *59*, 37-42.
[40] Frolov Yu.V., Pivkina A.N., Zav'yalov S.A., Preparation of Nanosized Particles of Energetic Substances, *Dokl. Phys. Chem.*, **2002**, *383*, 81-83.
[41] Herrmann M., Fietzek H., *Investigation of the Microstructure of Energetic Crystals by Means of X-ray Powder Diffraction*, International Centre for Diffraction Data 2005, Advances in X-ray Analysis, **2005**, *48*, 52-58.
[42] Xu R.-J., Kang B., Huang H., Chen Y., Jiang Y., Xia Y.-X., Nie F.-D., Characterization and Properties of Desensitized Octogen, *Chinese J. Explos. Propellants*, **2010**, *18*, 518-522.
[43] Jungová M., Zeman S., Husárová A., Friction Sensitivity of Nitramines. Part 1: Comparison with Impact Sensitivity and Heat of Fusion, *Chinese J. Energ. Mater.*, **2011**, *19*, 603-606.
[44] Zhang C., Understanding the Desensitizing Mechanism of Olefin in Explosives versus External Mechanical Stimuli, *J. Phys. Chem. C*, **2010**, *114*, 5068-5072.
[45] Liu Y.C., Wang J.H., An C.W., Yu Y.W., Effect of Particle Size of RDX on the Mechanical Sensitivity, *Chinese J. Explos. Propellants*, **2004**, *27*, 7-9.
[46] Song X., Wang Y., An C., Guo X., Li F., Dependence of Particle Morphology and Size on the Mechanical Sensitivity and Thermal Stability of Octahydro-1,3,5,7-tetranitro-1,3,5,7-tetrazocine, *J. Hazard. Mater.*, **2008**, *159*, 222-229.
[47] Larson T.E., Dimas P., Hannaford C.E., Electrostatic Sensitivity Testing of Explosives at Los Alamos, *Proc. 9th (International) Symposium on Detonation*, Portland, Oregon, **1989**, Vol-II, p. 1076-1083.
[48] Klapötke T.M., *Chemistry of High Energy Materials*, Walter de Gruyter GmBH and Co. KG, Berlin, New York, **2011**, p. 106.